Development 136, 1889-1898 (2009) doi:10.1242/dev.030866

Mechanical control of global cell behaviour during dorsal closure in *Drosophila*

Nicole Gorfinkiel[1,*], Guy B. Blanchard[2], Richard J. Adams[2] and Alfonso Martinez Arias[1]

Halfway through embryonic development, the epidermis of *Drosophila* exhibits a gap at the dorsal side covered by an extra-embryonic epithelium, the amnioserosa (AS). Dorsal closure (DC) is the process whereby interactions between the two epithelia establish epidermal continuity. Although genetic and biomechanical analysis have identified the AS as a force-generating tissue, we do not know how individual cell behaviours are transformed into tissue movements. To approach this question we have applied a novel image-analysis method to measure strain rates in local domains of cells and performed a kinematic analysis of DC. Our study reveals spatial and temporal differences in the rate of apical constriction of AS cells. We find a slow phase of DC, during which apical contraction of cells at the posterior end predominates, and a subsequent fast phase, during which all the cells engage in the contraction, which correlates with the zippering process. There is a radial gradient of AS apical contraction, with marginal cells contracting earlier than more centrally located cells. We have applied this analysis to the study of mutant situations and associated a particular genotype with quantitative and reproducible changes in the rate of cell contraction and hence in the overall rate of the process. Our mutant analysis reveals the contribution of mechanical elements to the rate and pattern of DC.

KEY WORDS: Apical contraction, Forces, Kinematic, Morphogenesis

INTRODUCTION

Morphogenesis is the process whereby cells reorganize in space to generate tissues and organs and, at a higher order level, organisms. Genetic studies have revealed that proteins involved in the regulation of the activity of the cytoskeleton and cell adhesion play a central role in morphogenesis. The information derived from these studies, coupled to the analysis of mutant phenotypes in time-lapse movies, has begun to give us some insights into the cellular basis of large-scale organization of tissues and organs (Bertet et al., 2004; Blankenship et al., 2006; Dawes-Hoang et al., 2005; Lecuit and Lenne, 2007). However, it is clear that an understanding of morphogenetic processes requires interrogating cells about how their genetic make-up is transformed into mechanical properties and thereby into coordinated dynamics that create reproducible tissue deformations over time. Here we use the process of dorsal closure (DC) of the *Drosophila* embryo as a system to understand how individual cell activities contribute to tissue behaviour in the context of a morphogenetic process.

Dorsal closure starts halfway through embryogenesis, when the epidermis exhibits an elliptically shaped discontinuity on its dorsal side that is bridged by the amnioserosa (AS), a squamous epithelium, continuous with the epidermis, that does not contribute to the larva (Jacinto et al., 2002b; Martinez Arias, 1993). The process requires a carefully choreographed sequence of cell-shape changes and interactions as contraction of the AS, coupled to convergence of the lateral epidermis towards the dorsal midline, progressively reduces and then eliminates the discontinuity and provides the embryo with its final shape. The AS, which lies on top of, and interacts with, a large cell called the yolk cell (Narasimha and Brown, 2004; Reed et al., 2004), uses apical contraction of its individual cells to reduce the global surface area of the tissue (Franke et al., 2005; Fernández et al., 2007; Homem and Peifer, 2008; Kiehart et al., 2000), while the epidermal cells elongate in the dorsoventral (DV) axis led by the dorsal-most epidermal cells, which exhibit specialized structure and behaviour (Kaltschmidt et al., 2002; Noselli, 1998; Ring and Martinez Arias, 1993; Stronach and Perrimon, 2001; Young et al., 1993). These cells assemble an actin-myosin cable at their dorsal-most edge (Edwards et al., 1997; Jacinto et al., 2002a; Kaltschmidt et al., 2002; Kiehart et al., 2000) that seeds cellular protrusions, filopodia and lamellipodia, which play adhesive and segment-matching roles in the late stages of DC (Jacinto et al., 2000; Liu et al., 2008; Millard and Martin, 2008). A number of studies have implicated interactions between the cytoskeleton and cell-adhesion systems in the development and coordination of these movements (Bloor and Kiehart, 2002; Fox et al., 2005; Franke et al., 2005; Gorfinkiel and Martínez Arias, 2007; Grevengoed et al., 2001; Magie et al., 2002; Murray et al., 2006; Takahashi et al., 2005). Furthermore, laser ablation of small groups of cells in the AS or the epidermis have revealed some of the forces involved in DC. In particular, these experiments show that the contraction of the AS and the tension in the supracellular actin-myosin cable contribute actively to the process, whereas the bulk of the lateral epidermis opposes closure (Hutson et al., 2003; Kiehart et al., 2000). The interface between the epidermis and the AS, the leading edge (LE), acts as a fulcrum for the convergence of the forces that define the rate and pattern of DC (Hutson et al., 2003; Kiehart et al., 2000; Peralta et al., 2008).

Although the elongation of epidermal cells makes a significant contribution to DC, the contraction of the AS is increasingly becoming a focus of attention as a major additional force driving the movement (Fernández et al., 2007; Kiehart et al., 2000; Lamka and Lipshitz, 1999; Scuderi and Letsou, 2005), and also as a system to read the mechanics of the process. Here we track AS cells individually and use a novel image-analysis method to measure strain rates in local domains of cells (Blanchard et al., 2009) to perform a kinematic analysis of DC. Our results reveal a degree of pattern and organization in the contraction of the AS not perceptible in previous studies and highlights a role for mechanical cues in the

[1]Department of Genetics, University of Cambridge, Downing Street, Cambridge CB2 3EH, UK. [2]Department of Physiology, Development and Neuroscience, University of Cambridge, Downing Street, Cambridge CB2 3DY, UK.

*Author for correspondence (e-mail: ng288@hermes.cam.ac.uk)

Accepted 31 March 2009

coordination of cell behaviour that is important for the pattern and efficiency of morphogenetic processes. Our study begins to unravel the way in which individual cells coordinate and integrate their activities to produce predictable patterns of behaviour at the tissue level.

MATERIALS AND METHODS

Drosophila strains

The following stocks were used in this study: ubiECadGFP (Oda and Tsukita), enGal4, enGal4 UASactinGFP, c381GAL4 (a GAL4 driver expressed in the AS), P0180 (expressed in yolk cell), UASp-35, UAS-TorsoDβPScyt, a dominant-negative adhesion form of βPS integrin (Martin-Bermudo and Brown, 1999), UAS-spastin-EGFP (Trotta et al., 2004) and myospheroid[1] (*mys*^{1}, an amorph allele for βPS integrin subunit). UAS lines were expressed using the Gal4 system (Brand and Perrimon, 1993). To identify mutant and overexpressing embryos, FM7, KrGFP and TM3, KrGFP balancers were used. When not stated otherwise, stocks were obtained from the Bloomington Stock Center.

Immunostainings

Embryos were fixed and stained as previously described (Kaltschmidt et al., 2002). For thick sections, the procedure described by Narasihma and Brown (Narasihma and Brown, 2004) was followed. The following primary antibodies were used: rabbit antisera against β-galactosidase (1/10000, Cappel), rabbit antisera against Bazooka (1/500, a gift from A. Wodarz), rat monoclonal against Ecad [DCAD2, 1/20, Developmental Studies Hybridoma Bank (DSHB), University of Iowa, developed by T. Uemura], rabbit antisera against Scribbled (1/2000, a gift from C. Doe). The following conjugated secondary antibodies were used: Alexa-fluor-488-, Alexa-fluor-568- and Alexa-fluor-647-conjugated antibodies from Molecular Probes and Alexa-fluor-568-conjugated phalloidin (Molecular Probes) for F-actin detection.

Time-lapse movies

Stage 13 *Drosophila* embryos carrying an ubiDECadherinGFP construct (Oda and Tsukita, 2001), which express a fusion between DECadherin and GFP, were dechorionated, mounted on coverslips with the dorsal side glued to the glass and covered with Voltalef oil 10S (Attachem). Imaging of the

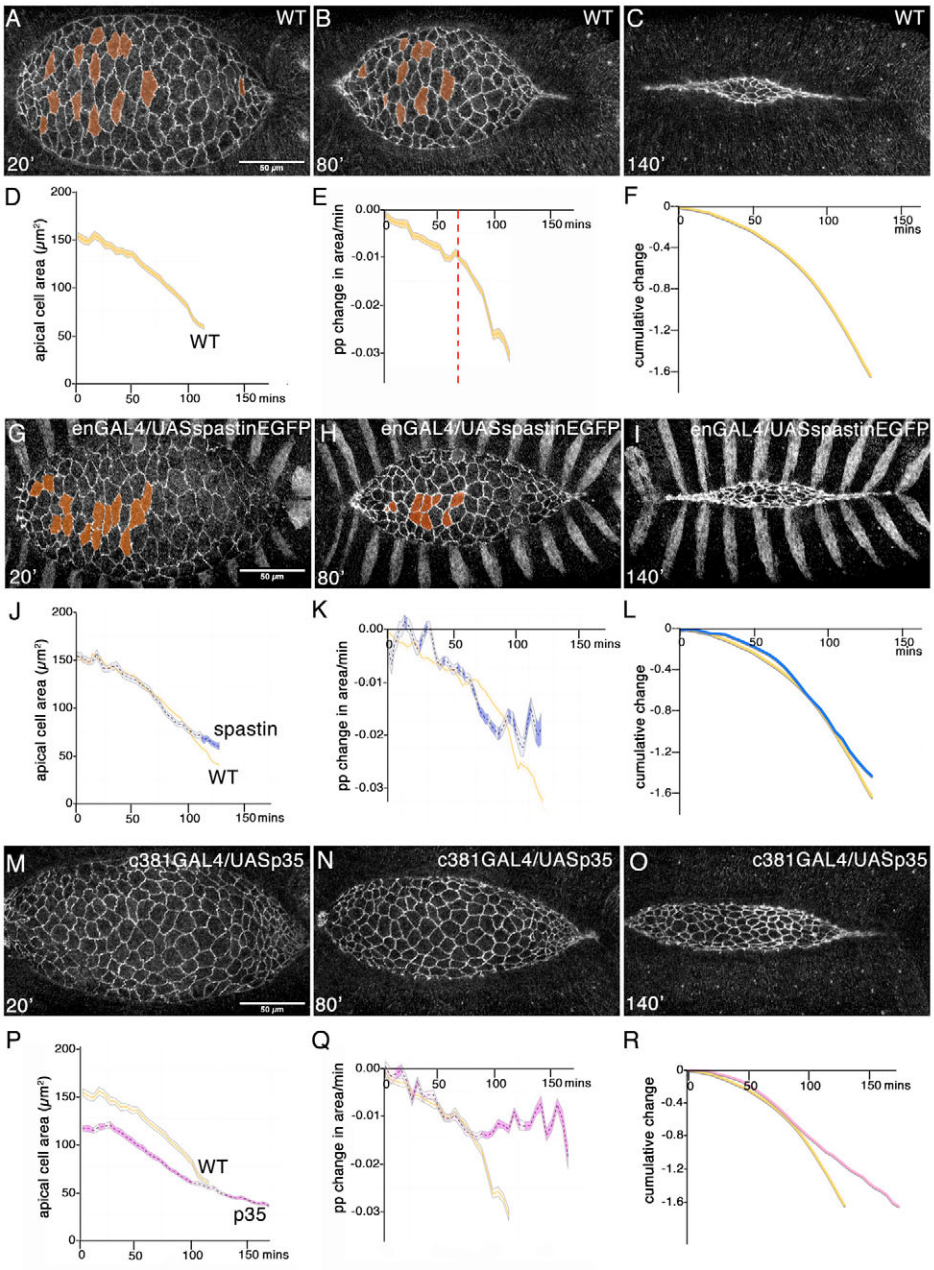

Fig. 1. Dynamics of amnioserosa contraction in pooled wild-type and mutant *Drosophila* embryos. (**A-C**,**G-I**,**M-O**) Still images from a time-lapse movie of a wild-type embryo (A-C; see Movie 1 in the supplementary material), an enGal4/UAS-spastin-EGFP embryo (G-I; see Movie 2 in the supplementary material) and an ASGal4/UAS-p35 embryo (M-O; see Movie 3 in the supplementary material), carrying the ubiECadGFP transgene at 20, 80 and 140 minutes after the start of dorsal closure (DC), defined as the onset of amnioserosa (AS) contraction. Anterior is to the left in these and all subsequent images. Cells that undergo basal extrusion (before being reached by the zippering epidermis) are labelled in red. (**D-F**) Data are pooled from four wild-type embryos (orange ribbons). Staging of embryos was by comparing the morphogenesis of the posterior spiracles. (**J-L**) Data are pooled from four different enGal4/UAS-spastin-EGFP embryos (blue ribbons). (**P-R**) Data are pooled from three different ASGal4/UAS-p35 embryos (magenta ribbons). For the shading code of the ribbons, see Materials and methods. (D,J,P) Mean apical cell area. (E,K,Q) Proportional rate of change in apical area of AS cells. In E, the transition from the slow phase (0-70 minutes) to the fast phase (70 minutes to end) is highlighted (dashed red line). (F,L,R) Cumulative proportional area change. Data from single embryos are shown in Fig. S1 in the supplementary material. Fluctuations in contraction rates in K and Q are considered to be noise due to experimental error and enhanced variability in the phenotype of mutant embryos (developmental timings are known to be more variable between mutants than between wild-type embryos). Although fluctuations in apical cell area do exist at early stages of development (data not shown), they occur on a smaller time scale than those shown in these graphs.

AS was done using an inverted LSM 510 Meta laser-scanning microscope with a 40× oil immersion Plan/Fluor (NA=1.3) objective. Embryos were maintained at 24°C during imaging and between 45 and 50 *z*-sections 1 μm apart were collected every 2 minutes, with the whole AS in view.

Cell tracking and data analysis

Automated cell tracking was performed using custom software written in Interactive Data Language (IDL, ITT). AS shape was determined by detecting the AS surface from its fluorescent signal. Curved image layers were extracted using these shapes and used to track cells over time based on the identification of cell membranes. Cells that showed abnormal tracking (i.e. unreasonable apical cell area, rate of area change or cell displacement, generally meaning that two or more cells have been fused during the tracking process) were not taken into account. Cells that touched the edge of the field of view were also excluded from the analyses because they may have been incomplete. We quantified the morphogenesis of the AS using strain rates that describe the rate of change in the shape of single cells. More precisely, a strain rate is the ratio of the change in size to the original size divided by the time interval. Mostly, we used the proportional rate of change in the area of a cell, also termed the dilatation strain rate, calculated as [Area(t+dt)–Area(t-dt)]/[Area(t) × 2 × dt], for a cell at time t, with t and dt in minutes. Where we were interested in the differential contribution of the dilatation rate in the anteroposterior (AP) and mediolateral (ML) orientations, we calculated strain rates as the proportional rates of change in cell size in each of these independent orientations. The mean of these strain rates is equal to the dilatation strain rate. We expressed the morphogenesis of multicellular aggregates as the area-weighted average of the strain rates of the contained single cells. For a detailed description of cell-tracking method and quantification of cell-shape changes, see Blanchard et al. (Blanchard et al., 2009).

The zippering phenotype was quantified by measuring the height and the width of the AS over time and the fitted constants, V (the relative velocity of the leading edge) and kz (the rate constant of zipping), were obtained using the rate-process model of DC (Hutson et al., 2003). Note that kz is a kinematic measure of the change in the shape of the AS and not a measure of the force of an active zippering process. We looked for an association between the zippering rate, kz, and the proportional rate of contraction of AS cells. We observed that the relationship between the proportional reduction in cell area versus time was approximately linear throughout the fast phase in all backgrounds, so we looked at the relationship between the gradients of these linear relationships and the rate of zippering. We first fitted a linear regression to the proportional area change/minute during the fast phase for each embryo, then plotted the gradients of these fits against kz.

Statistical validation

We constructed a mixed-effects model (Pinheiro and Bates, 2000), using R (R Development Core Team, 2005) to test for evidence of differences between data derived from different embryos. We estimated the *P*-value associated with a fixed effect of differences between genotypes, allowing for random effects contributed by differences between embryos within a given genotype. Error ribbons show the typical standard error for data from one embryo, averaged across all embryos of that group. Sections of ribbons are shaded when $P<0.05$, signifying evidence for a difference between genotypes (Wickman, 2008).

RESULTS

Dynamics of AS contraction

During DC, the AS progressively reduces its surface area through the apical contraction of individual AS cells (Kiehart et al., 2000). It is known that these cells reduce their apical surface area at the same rate as the AS changes shape as a whole (Kiehart et al., 2000), but these studies do not provide information about how individual cell behaviours contribute to the ordered contraction of the tissue. To obtain this information we have used time-lapse movies of wild-type embryos labelled with an apical membrane marker (ECadGFP) (Fig. 1A-C; see Movie 1 in the supplementary material) to track all individual AS cells automatically and quantify tissue deformation and cell-shape changes, applying a recent developed analytical method (Blanchard et al., 2009).

The AS contains 187±18 (n=9) cells, which contract their apical surface areas continuously from shortly after germ band retraction until the end of DC (Fig. 1D), with negligible contribution of cell intercalation (Blanchard et al., 2009). About 10% of AS cells drop out basally of the plane of the epithelium (Kiehart et al., 2000) (Fig. 1A-C; see Table S1 in the supplementary material), a loss that further contributes to the decrease in AS surface area. Our analysis of the average rate of apical contraction of AS cells reveals two distinct phases: one characterized by a slow increase in the rate of contraction and a second, rapidly increasing, faster phase (Fig. 1E). We observe that the transition from the slow to the fast phase of contraction coincides with the engagement of the anterior canthus, which always lags 35/40 minutes behind the posterior one. The formation of canthi, which engage the two epidermal sheets at the anterior and posterior ends of the AS to initiate the zippering of the epidermis, is a significant event in DC (Jacinto et al., 2002b).

These data suggest the existence of a correlation between the zippering rate and AS cell contraction. If this correlation were causal, slowing the zippering process would affect the rate of contraction of AS cells. To test this we triggered a delay in the zippering process by expressing an EGFP-tagged version of the microtubule-severing protein Spastin specifically in the epidermis (Fig. 1G-L; see Movie 2 in the supplementary material) (Jankovics and Brunner, 2004). Quantification of the zippering rate in these

A

Genotype	kz (nm/sec)	gradient of pp change in area/min
ubiECadGFP	19.83	-0.0005
	17.33	-0.0003
	27.12	-0.0005
	18.83	-0.0007
enGal4/UAS-spastin-EGFP	14.83	-0.0002
	13.83	-0.0003
	12	-0.00003
	14.8	-0.00003
ASGal4/UAS-p35	8.83	0.00005
	7.17	-0.00005
	6.67	0.00004
mys	3.5	0.00005
	3.5	0.00004
	3.8	-0.00003
	3.8	0.00009

B

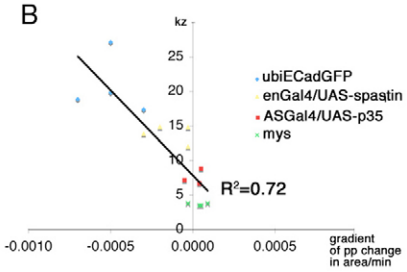

Fig. 2. Correlation between the zippering rate and the rate of contraction of AS cells. (**A**) Zippering rate (kz) and gradient of proportional change in area/minute (see Materials and methods) for the different embryos analysed. There are significant differences in the kz and in the gradient of proportional change in area/minute between wild-type and enGal4/UAS-spastin *Drosophila* embryos (kz: t=3.04, df=6, *P*=0.023; gradient of proportional change in area/minute: t=–3.41, df=6, *P*=0.014) as well as between wild-type and ASGal4/UAS-p35 embryos (kz: t=5.02, df=5, *P*=0.004; gradient of proportional change in area/minute: t=–5.12, df=5, *P*=0.004) and between wild-type and *mys* embryos (kz: t=7.87, df=6, *P*<0.001; gradient of proportional change in area/minute: t=–6.13, df=6, *P*<0.001). (**B**) The relationship between these two measures, using linear regression.

embryos (Hutson et al., 2003) shows that they exhibited an average zippering rate of 13.9 nm/second (n=4), which is significantly slower than the 20.8 nm/second (n=4) exhibited by ubiECadGFP embryos (Fig. 2A). In these embryos, AS cell contraction proceeded normally through most of the slow phase. However, the fast phase started earlier than in the wild type, and AS cells, instead of increasing their rate of apical contraction, continued to contract at a constant rate (Fig. 1J-L).

To analyze this further, we looked for a correlation between the increase in the rate of AS cell apical contraction during the fast phase and the zippering rate. We expect zippering to become an increasingly significant input on the rate of AS contraction as the AS gets smaller and canthi angles are reduced, because of the proportional increasing length of leading edge cells that can make filopodial contact across the AS. As a measure of the gradual increase in the rate of apical contraction, we calculated the gradient of the proportional reduction in cell area during the fast phase for each embryo (see Materials and methods; Fig. 2A). This parameter illustrates further the significant differences in the dynamics of the rate of AS cell contraction between wild-type and enGal4/UAS-spastin embryos (Fig. 2A). Moreover, we found a strong association between the zippering rate and the increase in rate of apical contraction of AS cells (Fig. 2B), suggesting that these two processes are interdependent (see below).

Another event that might play an important role in DC is the elimination of cells, which begins at the canthi during the onset of the zippering process, and is also observed in more centrally located regions (Fig. 1A-C). To analyze this possibility we inhibited apoptosis and completely prevented the associated cell extrusion in the AS by expression of the caspase inhibitor p35 (ASGal4/UAS-p35) (Fig. 1M-R; see Table S1 and Movie 3 in the supplementary material). At the onset of DC, these embryos had more AS cells (228±23, n=4) than wild-type ones, even though their average apical cell area was smaller (Fig. 1M). This indicates that apoptosis is a constant effector of global size regulation in this tissue and that cell area adjusts to the total number of cells. ASGal4/UAS-p35 embryos also exhibited a delay in the zippering movements (Fig. 1O) but eventually completed closure after a long delay (approximately 1 hour) and 3% (n=130) exhibit anterior holes in the cuticles (data not shown). These embryos had an average zippering rate of 7.6 nm/second (n=3), almost three times slower than that of ubiECadGFP embryos (Fig. 2A), and lacked a clear fast phase of AS cell contraction (Fig. 1Q,R). The gradient of the proportional reduction in apical cell area versus time of these embryos (Fig. 2A) correlates with their zippering rate (Fig. 2B), confirming the association between these two processes.

These results show that the zippering process affects the dynamics of apical contraction of AS cells, and reciprocally, that interfering with the dynamics of AS cell contraction affects the rate of zippering. The strong association between the increase in the rate of apical cell contraction and the zippering rate across different mutants confirms the tight interplay between these two processes.

Anisotropies in AS cell apical contraction

The contraction of the AS is not an isotropic process (Fig. 3) (Kiehart et al., 2000). We observed that for most of the time contraction was achieved by a decrease of the apical cell area in the ML direction only, and once the fast phase had engaged, the rate of ML increased and a small AP contraction was detected (Fig. 2A,B). This preferential contraction in the ML direction suggests that apical contraction is polarized in the plane of the epithelium. Recent studies have shown that during germ-band extension AS cells display planar polarity, as revealed by the preferential localization of the polarity protein Bazooka (Baz) at dorsoventral cell contacts and of Myosin II at the AP ones. This planar polarity of AS cells is associated with the cell-shape changes that occur early in this tissue (Pope and Harris, 2008). At the onset of DC, the polarized localization of Baz is lost and instead AS cells exhibit an inhomogenous distribution around the membrane (see Fig. S2 in the supplementary material), which does not correlate with the more homogeneous distributions of myosin, actin (data not shown) or DECad (see Fig. S2 in the supplementary material). These findings suggest to us that the polarized contraction of AS cells that we observe is unlikely to be driven by the local subcellular regulation of cytoskeletal and adhesion components, and that it is mainly the result of extrinsic mechanical constraints of the tissue.

In contrast to ML contraction, the contribution of contraction in the AP direction to global AS-cell apical contraction only manifested itself once the fast phase had begun, suggesting that it is a consequence of the zippering movements. In support of this, we noticed that in ASGal4/UAS-p35 embryos the contraction in AP started at the same time as the wild type and then continued for as long as the zippering process went on (see Fig. S3 in the supplementary material). This observation indicates that zippering movements are associated with apical cell contraction in the AP orientation and that the behaviour of AS cells is a result of a combination of AS intrinsic forces and external constraints.

Regional differences in the dynamics of contraction: the canthi

Average cell behaviours are useful to describe the dynamic properties of a tissue, but they mask differences between individual cells, or cell ensembles, that sustain the mechanisms underlying those dynamic properties. For example, there is evidence that during DC the cells at the canthi behave differently from the rest as they begin their contraction before the centrally located cells (Fernández et al., 2007; Harden et al., 2002). To analyze in more detail spatial differences in the behaviour of AS cells, we generated a system of coordinates to identify cells along the AP and ML axes of the embryo (–100 μm corresponds to the most anterior cells of the AS). Our quantitative analysis revealed that posterior canthi cells were the first ones to contract their apical surface area in both ML and AP directions (Fig. 4A,B,B′), followed by anterior canthi cells (Fig. 4A,C,C′). These localized apical contractions underlie most of the

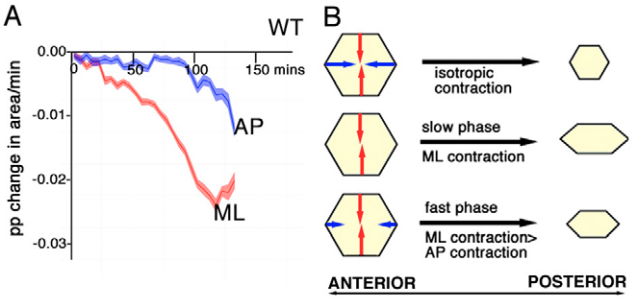

Fig. 3. Preferential apical contraction of AS cells in the mediolateral axis. (**A**) Proportional rates of size change of AS cells in mediolateral (ML, red) and anteroposterior (AP, blue) orientations for data pooled from four wild-type *Drosophila* embryos. (**B**) Schematic of data from A. Only towards the end of DC is there a significant AP-oriented contribution to apical cell contraction. Ribbons show mean±s.e.

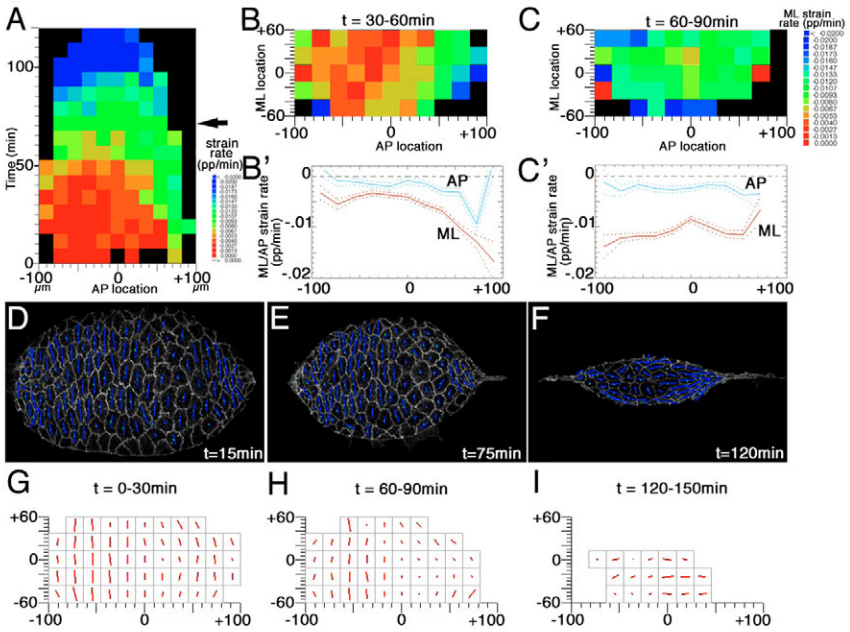

Fig. 4. Differences in cell behaviour along the AP axis in wild-type *Drosophila* embryos. (**A**) Proportional change in area/minute (area strain rate) of AS cells as a function of their AP location over time. The arrow indicates the transition between the slow and the fast phases. (**B**,**C**) Mean proportional rates of change in the ML orientation for cells across the AS for the periods 30-60 minutes and 60-90 minutes after the start of dorsal closure, respectively. Colours represent the mean behaviour of cells that fall within each tile of AS tissue. (**B′**,**C′**) The same data as in B,C are presented as averages over the ML (red) and the AP (light blue) axis, for the same periods of DC. Data are pooled from four wild-type embryos in all graphs. (**D-F**) Still images from an animation of an example wild-type embryo, showing the relative magnitude and orientation of the long axis of AS cells. (**G-I**) Cell orientation data are pooled from four aligned wild-type embryos, and regional averages are shown for three epochs of DC: 0-30, 60-90 and 120-150 minutes after the onset of DC. The orientation of the red lines represents the mean (elongation ratio-weighted) orientation of the long axis of cells in each grid square. The lengths of red lines represent the elongation log-ratio of the long to short axes of cell shapes. A line length equal to the size of a grid square equals a log-ratio of 1.0 (a ratio of 2.718:1).

slow phase and towards the end, all AS cells engaged in the contraction of their apical surface in the ML direction with little contribution of AP apical contraction (Fig. 4A,C,C′). In addition to these AP differences in the rate and preferred direction of apical contraction, anterior and posterior cells exhibited shape differences, as shown by the evolution of the orientation and magnitude of their long axis (Fig. 4D-I). During most of the slow phase, all cells had this axis orientated perpendicular to the AP axis of the embryo (Fig. 4D,G), but shortly before the onset of the fast phase, posterior cells began to orientate their long axis parallel to the embryo AP axis while anterior cells still orientated perpendicular to it (Fig. 4E,H). Later on, anterior cells also oriented their long axis parallel to the embryo AP axis, although in a more uncoordinated manner (Fig. 4F,I). These inhomogeneities in the rate of apical cell contraction and cell shape along the AP axis were also observed in enGal4/UAS-spastin (data not shown) and ASGal4/UAS-p35 embryos (see Fig. S4 in the supplementary material). However, in these embryos the degree of elongation of AS cells along the ML direction during the slow phase of DC was lower than in wild-type ones (compare Fig. 4G,H with Fig. S4F,G in the supplementary material). We attribute these differences to the need to accommodate a higher number of AS cells in ASGal4/UAS-p35 embryos. In spite of these differences in cell shape, the relative contributions of AP and ML contraction were not altered in these embryos compared to wild-type ones (see Fig. S3 in the supplementary material), suggesting that the rate of apical cell contraction is independent of cell shape.

Such dynamic spatial patterning of the apical contraction of AS cells is probably not a direct consequence of a corresponding dynamic pattern of differential gene expression. In our view, it is more probable that these patterned differences in cell behaviour are a consequence of variations in the mechanical environment across the AS. For example, the anterior two-thirds of the AS cells lie on top of the yolk and are attached to it through integrin-mediated adhesion, whereas posterior cells lie free on top of the gut (Narasimha and Brown, 2004; Reed et al., 2004). This differential attachment could create differential constraints determining differential cell behaviour. For example, there is a region of the AS that coincides with the limit of the underlying yolk where cells are more isometric and larger than in the rest of the tissue (Fig. 4D,G, cells between +10 and +60 μm), suggesting that the presence or absence of a physical support influences cell shape. Also, at the anterior end, head involution occurs in parallel to DC and it has been suggested that this contributes to AP inhomegeneities in the geometry of closure (Peralta et al., 2007). Interestingly, AS cells that are extruded from the plane of the epithelium before being reached by the advancing canthi (i.e. central cells that are extruded) are mostly detected in the anterior half of the embryo (see Fig. 1A,C). This observation suggests to us that the differential mechanical constraints on the AS along the AP axis contribute to the observed pattern of cell behaviours (rate of apical contraction, shape and extrusion).

Regional differences in the dynamics of contraction: a gradient of AS contraction

The marginal cells of the AS have been shown to begin their contractions before the more centrally located cells (Fernández et al., 2007; Lamka and Lipshitz, 1999; Wada et al., 2007). This observation led us to analyse whether there is a gradient of contraction from the

leading edge towards the centre of the AS. To do this, we generated a system of radial coordinates to identify cells according to their position relative to the margin. The radial coordinate of a cell varies from 0 at the centre of the AS to 1 at the edge of the AS, irrespective of its location along the body axes. Analysis of the rate of AS cell apical constriction along this radial coordinate system reveals a gradient of contraction from the leading edge towards the centre, with peripheral cells contracting faster than centrally located cells (Fig. 5A,A′). This gradient starts to develop during the slow phase and is maintained throughout most of the fast phase.

A model in which a signal emanates from the epidermis could explain the radial pattern of apical contraction in the AS. Dpp signalling from the epidermis has been shown to be required for AS (Fernández et al., 2007) and thus would be a candidate for such a signal. However, enGal4/UAS-spastin and ASGal4/UAS-p35 embryos, in which the zippering rate was affected without perturbing signalling, did not develop a proper radial pattern of apical cell contraction in the AS (Fig. 5B-C′). Although this does not eliminate the possibility that Dpp contributes to the gradient of contraction, it adds further support for a mechanical component provided by the zippering force that influences the patterning of the AS.

These results, together with the average and anisotropic properties of the AS described above, indicate the existence of regional differences in the activity of the AS cells that are determined by their physical environment. The epidermis, the yolk cell and other morphogenetic processes that occur concomitant with dorsal closure are likely to contribute to this environment. Moreover, it is the coordination in space and time of these regional behaviours that gives rise to the patterns of contraction within the AS.

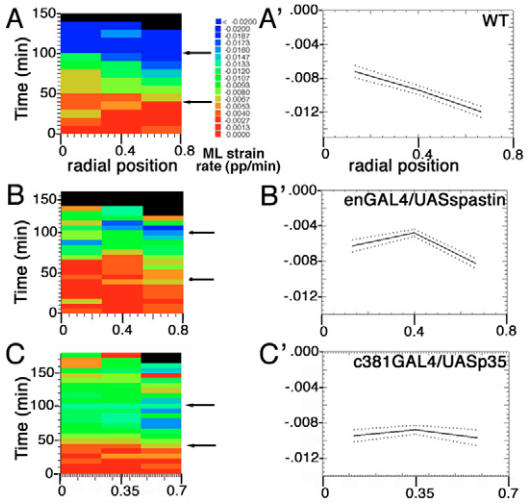

Fig. 5. A gradient of AS cell contraction from the leading edge towards the dorsal midline depends on the zippering of the epidermis. (**A-C**) Proportional rates of change of cell shape in the ML orientation summarized by radial location. Cells at both canthi are removed from this analysis because they are known to be directly affected by zippering. Data are pooled from four wild-type (A), four enGal4/UAS-spastin-EGFP (B) and three ASGal4/UASp35 (C) *Drosophila* embryos. Note the 'stair-like' distribution of shape strains in A, indicating that external cells are contracting their apical surface areas faster and earlier than central cells. (**A′-C′**) The same data as in A-C presented as time averages for 40-100 minutes after the onset of DC (arrows in A-C). In enGAL4/UAS-spastin embryos, there is only a peripheral gradient of apical contraction, whereas in ASGal4/UAS-p35 embryos there is no gradient of apical contraction along the radial axis (all cells contract at approximately the same rate).

The zippering process integrates different cellular activities

Traditionally, mutants are used to infer the wild-type functions of a gene from the phenotype of its lack of function. However, in the context of morphogenesis, mutants can be construed as perturbations of the function of a complex system that provide insight into a coordinated activity (Glickman et al., 2003; Hutson et al., 2003). Here we have adopted this strategy and used mutants in *myospheroid* (*mys*) to test the contribution of particular cellular activities to dorsal closure. These mutants lack the integrin βPS subunit (Brown, 1994), a cellular receptor involved in cell-extracellular matrix and cell-cell interactions, and exhibit problems during DC: the AS detaches from the underlying yolk cell, and in the late phase of the process the epidermis separates from the AS (Homsy et al., 2006; Narasimha and Brown, 2004; Peralta et al., 2007; Reed et al., 2004; Wada et al., 2007). A biomechanical analysis based on the dynamic geometry of closure has predicted that the zippering of the epidermis is impaired in these mutants before the epidermis and AS rip themselves apart (Hutson et al., 2003).

Time-lapse movies of *mys* zygotic embryos expressing the ubiCadGFP construct confirmed that DC in these embryos was slower than in wild type (Fig. 6A; Fig. 5F; see Movie 4 in the supplementary material). The first clear defect of the loss of Mys was the delay in the formation of the canthi and the zippering movements, which initiated, albeit at a slower rate, and then proceeded with difficulty. In these embryos, epidermal cells exhibited normal filopodia on the dorsal side of the DME cells (Fig. 6G; see Movie 5 in the supplementary material), which suggests that the zippering defects cannot be attributed to problems in the interactions between epidermal cells. Furthermore, the percentage of extruded cells, as well as their preferential anterior location, was normal (see Table S1 in the supplementary material; Fig. 6A-C), indicating that the zippering defects in *mys* embryos are not a consequence of abnormal apoptosis-mediated cell extrusion. At later stages the epidermis detached from the AS, then continued its contraction autonomously with many of the wild-type features (Fig. 6D-F).

It has been suggested that the yolk is required for normal AS contraction and that some of the abnormalities of DC in *mys* mutants can be traced to this defect (Narasimha and Brown, 2004). To test this we made use of embryos in which a dominant-negative form of the integrin βPS subunit is expressed in the yolk cell (Martin-Bermudo and Brown, 1999; Narasimha and Brown, 2004). In these embryos, P0180/UAS-TorsoβPScyt, only the attachment of the AS with the yolk was disrupted (Narasimha and Brown, 2004) (see Fig. S5 in the supplementary material), there were no obvious detachments between the AS and the epidermis and the zippering was not affected (Fig. 6H,I; see Movie 6 in the supplementary material). These observations suggest that the defects observed in *mys* embryos might be a composition of several weaker effects. Thus defects triggered by the loss of attachment between the AS and the epidermis might amplify and be amplified by a weaker yolk-cell-AS interface, which by itself does not cause a phenotype.

Mutants in *myospheroid* perturb the dynamics of AS contraction

Morphometric analysis revealed that in *mys* mutant embryos, although the beginning of AS contraction was delayed, the slow phase proceeded normally, and instead of entering the fast phase, AS

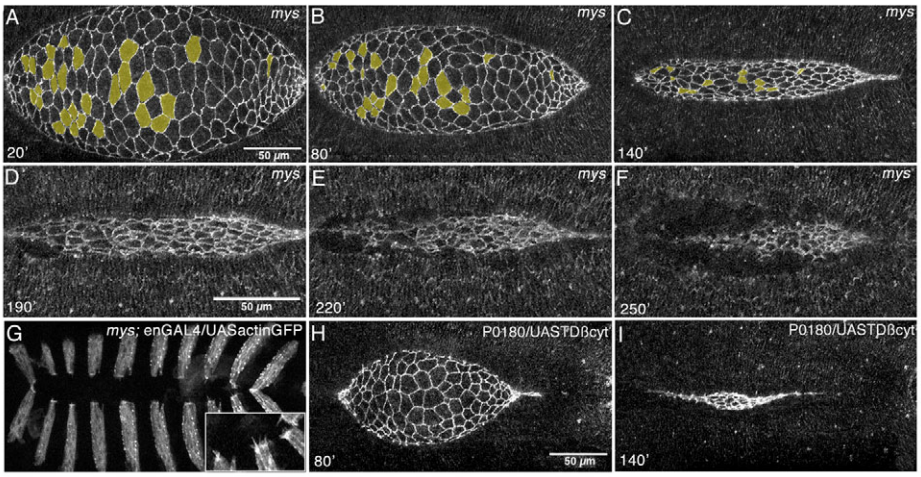

Fig. 6. Zippering defects in *mys* mutant *Drosophila* embryos is not a consequence of defective filopodia, lack of cell extrusion or attachment to the yolk. (**A-F**) Still images from a time-lapse movie of a *mys* mutant embryo carrying the ubiECadGFP transgene (see Movie 4 in the supplementary material) at 20, 80, 140, 190, 220 and 250 minutes after the onset of DC. After the epidermis and the AS tear apart, the AS keeps on contracting (D-F). (**G**) Image from a time-lapse movie of a *mys* mutant embryo carrying the enGal4 and UASactinGFP transgenes (see Movie 5 in the supplementary material). Dorsal-most epidermal cells form filopodia at their dorsal end (inset). (**H**,**I**) Still images from a time-lapse movie of a P0180/UAS-TorsoβPScyt embryo carrying the ubiECadGFP transgene (see Movie 6 in the supplementary material) at 80 and 140 minutes after the onset of DC. When expressed in wing imaginal discs, this construct produces blistering of the wing (Dominguez-Gimenez et al., 2007) (data not shown).

cells continued to contract at a constant, slow-phase rate (Fig. 7A-C). This slower rate of apical cell contraction correlates strongly with the slow zippering rate of these embryos (Fig. 2), in which apical contraction of AS cells occurred in the ML axis only (Fig. 7D) with almost no reduction of the apical cell surface area in the AP axis. These observations provide additional support to the correlation between the zippering process and the increasing rate of AS cell contraction during the fast phase.

At first sight, the dynamics of the AS in *mys* embryos appears to be a consequence of their strong zippering defects. However, the analysis of regional differences in cell behaviour in these embryos revealed additional features that may be indicative of the forces acting on the system. For example, in contrast to the behaviour of wild-type embryos, in which contraction of anterior cells dominates that of posterior cells by mid-DC, in *mys* embryos posterior cells always contracted faster than anterior cells (see Fig. S6 in the supplementary material). More surprisingly, the central AS cells of *mys* mutants reached faster rates of ML contraction than those of more external ones, as shown by an inversion of the radial gradient of apical cell contraction (Fig. 7E,F). One possible explanation for the faster rate of contraction of central cells could be a consequence of cell extrusion still occurring in *mys* embryos but not in ASGal4/UAS-p35 ones (see Table S1 in the supplementary material). Three lines of evidence suggest to us that cell extrusion is not the only contributing factor to the faster rates of ML contraction observed in these embryos. Firstly, enGal4/UAS-spastin embryos, which show normal cell extrusion (see Table S1 in the supplementary material), did not show this inversion of the radial gradient of AS cell contraction. Secondly, we observed that posterior cells in *mys* embryos also showed a higher rate of apical cell contraction than their wild-type or ASGal4/UAS-p35 counterparts (see Fig. S6 in the supplementary material), but cell extrusion occurred mainly at the anterior half of the AS (Fig. 6A-C). Finally, when we virtually removed the extruded cells from our analysis of AS dynamics, we observed that posterior and central cells still showed faster rates of ML contraction (see Fig. S7 in the supplementary material).

Thus, our results demonstrate differences in the intrinsic activity of cells in *mys* versus enGal4/UAS-spastin and ASGal4/UAS-p35 embryos. Because the high rate of apical cell contraction in *mys* embryos goes against the slowing down of the zippering speed, we would like to suggest that the faster rates of apical contraction observed in central and posterior AS cells from *mys* embryos are a consequence of the weakening of the epidermis-AS interface leading to a weakening of the resistance generated by the epidermis. Further support for this comes from the observation that in *mys* embryos the AS can still contract after the epidermis has detached from the AS (Fig. 6D-F), revealing an autonomous activity of the tissue that is normally counteracted by the resistance of the epidermis. An autonomous contraction of the AS is also observed in mutants for Ecad (Gorfinkiel and Martínez Arias, 2007), which show early detachments of the AS from the epidermis. Thus, our work provides in vivo evidence for the role of mechanics in the control of cell behaviour during morphogenesis.

DISCUSSION

The process of dorsal closure provides a good system to explore the relationship between cell biology and tissue mechanics and the way this informs morphogenesis. There are sound descriptions of the molecular and cellular events underpinning the process (Jacinto et al., 2002b), a large collection of mutants that interfere with the different stages (Harden, 2002), and some of the macroscopic forces underlying DC have been identified (Hutson et al., 2003; Kiehart et al., 2000; Toyama et al., 2008). Notwithstanding this, most of the studies have focused on the consequence that the loss of a gene has for the process. For this reason, an understanding of how individual cell behaviours contribute to the global patterning in the wild type is lacking. Here, we have begun to approach this problem by focusing on the AS, a genetically homogeneous tissue, the contraction of which provides a component of the force that drives closure.

Our study reveals that AS cell contraction is patterned in space and in time. At present there are no reports of differences in gene expression between different AS cells during DC, and therefore it is

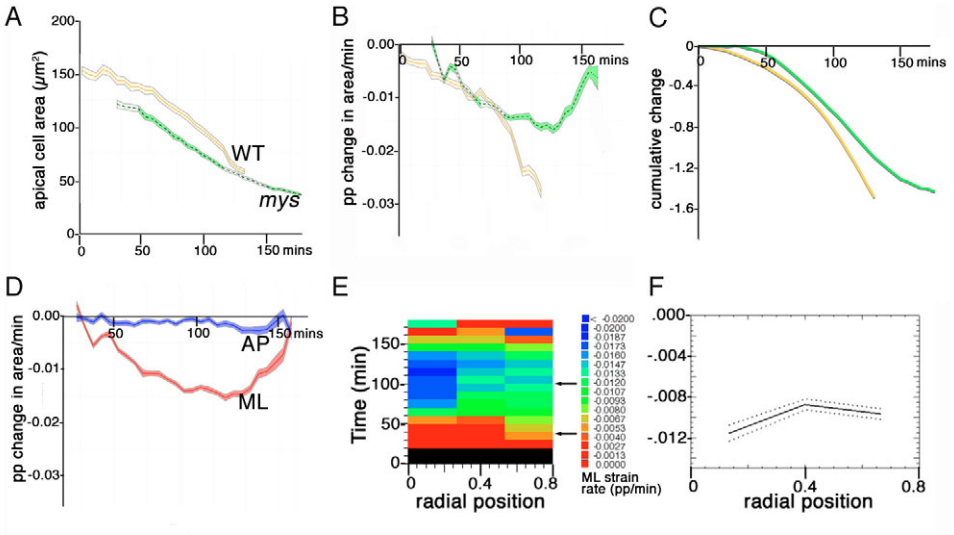

Fig. 7. Dynamics of AS contraction in *mys* mutant *Drosophila* embryos. (**A**) Mean apical cell area. (**B**) Proportional change in apical area. (**C**) Cumulative proportional area change. Data are pooled from four aligned *mys* embryos (green ribbons), with wild-type (orange) and ASGal4/UASp35 (magenta) ribbons presented as in Fig. 1. Both ASGal4/UASp35 and *mys* embryos lack a fast phase of AS contraction (B). (**D**) Proportional rates of size change of AS cells in ML (red) and AP (blue) orientations for data pooled from four *mys* embryos. (**E**,**F**) The radial pattern of ML-oriented cell shape strain rates is shown as in Fig. 4 for pooled *mys* data. Central cells contract their apical surface area in the ML orientation faster than peripheral cells during the period of 40-100 minutes.

unlikely that the complex dynamics that we have observed can be related to patterned gene activity. On the basis of our results, in particular the strong correlation between the zippering speed and the rate of contraction of the AS, we favour the possibility that the behaviour of the AS during DC is governed by mechanical interactions with its environment. Additional evidence for the role of cell mechanics in the process comes from the AP differences in the rate of contraction of AS cells and their patterns of shape changes, as well as the timing of individual contractions in the ML and AP axes, which are indicative of different stresses along the AP axis of the embryo. Thus, although AS cell contraction is triggered by Dpp signalling (Fernández et al., 2007), our work suggests that this might create a plastic state that is patterned by the integration, at the single cell level, of global mechanical cues. A role for mechanical cues in determining cell behaviour and cell fate has been shown for different cell types in cell culture (Chen et al., 1997; Engler et al., 2006; McBeath et al., 2004) and has been postulated to be an important regulator of morphogenetic movements (Ingber, 2006). The morphogenetic alterations discussed above, together with quantitative changes in the geometry of cell-cell contacts during DC (data not shown) suggest that adhesive and cytoskeletal properties of AS cells are modulated during the process through a combination of chemical and mechanical signals.

The two phases of activity of the AS cells revealed by our analysis are divided by the onset of epidermal zippering during which the filopodial activity developed by dorsal-most epidermal cells makes a significant contribution to the fusion and matching of the opposite epidermal flanks (Jacinto et al., 2000; Jankovics and Brunner, 2006; Millard and Martin, 2008). Our analysis shows that perturbing the zippering process, through interference of microtubule dynamics in the epidermis, affects the rate of contraction of AS cells, and, reciprocally, that perturbing the dynamics of AS contraction through inhibition of apoptosis-mediated extrusion affects the zippering rate. These observations support an interdependence between these two processes that is manifest in the correlation between the zippering rate and the dynamics of the rate of apical AS cell contraction. Recent work from Edwards, Kiehart and colleagues (Toyama et al., 2008) has also shown that inhibiting or enhancing apoptosis in the AS changes the kinematic properties of the closure, i.e. the rate of closure, the rate of zipping and the force produced by the AS. However, in contrast to our interpretation, the authors suggest a direct and causal relationship between apoptosis and the force generation in the AS. In the light of our results, we surmise that the changes in the force-generating capability of AS cells observed in their experiments are a secondary consequence of the effects of apoptosis on the zippering, which thus feeds back onto the AS. Cell extrusion is indeed an important contributor to the normal rates of DC, but our work suggests that it is an event that responds to, rather than directs, the strains of the whole AS.

Our study also demonstrates that assigning functions to particular genes during morphogenesis might be misleading. As we have shown here, the phenotype of a mutant during dorsal closure is not a direct consequence of the loss of function of a particular gene but the outcome that this loss of function has on a series of related cellular activities. In higher-order processes, such as morphogenesis, the result of a mutation is an array of perturbations acting at different levels of organization, which makes it difficult to infer a direct causal relationship between the mutated gene and the terminal phenotype (Noble, 2008). Acknowledging this, the system-level analysis we have performed here shows a correlation of a particular genotype with a reproducible change in the dynamics of the process, revealing the contribution of each gene product to the overall function.

Morphogenetic processes require complex spatiotemporal integration of cellular activities that results in patterns of activity at the tissue level. The behaviour of the AS during DC provides a simple system in which to begin to unravel the nature and levels of this integration and the manner in which chemical, mechanical and genetic inputs pattern the behaviour of an epithelium. To do this we have used a method that allows measurement of the deformation of individual cells and of tissue domains (Blanchard et al., 2009), and made use of mutants to perturb the system in a defined and

controlled manner. Our study reveals that regular patterns of tissue behaviour emerge from the short-range coordinated behaviour of individual cells upon which chemical signals and mechanical constraints are impressed from surrounding tissues. Our results highlight the importance of looking at the dynamics of cell populations, which cannot be obtained from the behaviour of individual cells.

Physical models have recently been applied to recapitulate the appearance of higher-order tissue architectures in different epithelia from the mechanical properties of individual cells (Farhadifar et al., 2007; Hilgenfeldt et al., 2008; Kafer et al., 2007; Rauzi et al., 2008). Kinematic quantitative analyses like the one we have presented here do provide the basis on which to build computational simulations of morphogenetic processes that will allow us to integrate the activity of genes, signals and mechanical properties into the behaviour of tissues.

This work was supported by a BBSRC grant to A.M.A., a BBSRC grant to A.M.A. and N.G. and an MRC grant to R.A. We are very grateful to members of our laboratories for fruitful discussions. N.G. thanks Lola Martín-Bermudo for the UAS-TorsoDβPScyt stock, and Carlos Torroja for discussions and support. Deposited in PMC for release after 6 months.

Supplementary material

Supplementary material available online at
http://dev.biologists.org/cgi/content/full/136/11/1889/DC1

References

Bertet, C., Sulak, L. and Lecuit, T. (2004). Myosin-dependent junction remodelling controls planar cell intercalation and axis elongation. *Nature* **429**, 667-671.

Blanchard, G. B., Kabla, A. J., Schultz, N. L., Butler, L. C., Sanson, B., Gorfinkiel, N., Mahadevan, L. and Adams, R. J. (2009). Tissue tectonics: morphogenetic strain rates, cell shape change and intercalation. *Nat. Methods* (in press).

Blankenship, J. T., Backovic, S. T., Sanny, J. S., Weitz, O. and Zallen, J. A. (2006). Multicellular rosette formation links planar cell polarity to tissue morphogenesis. *Dev. Cell* **11**, 459-470.

Bloor, J. W. and Kiehart, D. P. (2002). Drosophila RhoA regulates the cytoskeleton and cell-cell adhesion in the developing epidermis. *Development* **129**, 3173-3183.

Brand, A. H. and Perrimon, N. (1993). Targeted gene expression as a means of altering cell fates and generating dominant phenotypes. *Development* **118**, 401-415.

Brown, N. H. (1994). Null mutations in the alpha PS2 and beta PS integrin subunit genes have distinct phenotypes. *Development* **120**, 1221-1231.

Chen, C. S., Mrksich, M., Huang, S., Whitesides, G. M. and Ingber, D. E. (1997). Geometric control of cell life and death. *Science* **276**, 1425-1428.

Dawes-Hoang, R. E., Parmar, K. M., Christiansen, A. E., Phelps, C. B., Brand, A. H. and Wieschaus, E. F. (2005). folded gastrulation, cell shape change and the control of myosin localization. *Development* **132**, 4165-4178.

Dominguez-Gimenez, P., Brown, N. H. and Martin-Bermudo, M. D. (2007). Integrin-ECM interactions regulate the changes in cell shape driving the morphogenesis of the Drosophila wing epithelium. *J. Cell Sci.* **120**, 1061-1071.

Edwards, K. A., Demsky, M., Montague, R. A., Weymouth, N. and Kiehart, D. P. (1997). GFP-moesin illuminates actin cytoskeleton dynamics in living tissue and demonstrates cell shape changes during morphogenesis in Drosophila. *Dev. Biol.* **191**, 103-117.

Engler, A. J., Sen, S., Sweeney, H. L. and Discher, D. E. (2006). Matrix elasticity directs stem cell lineage specification. *Cell* **126**, 677-689.

Farhadifar, R., Roper, J. C., Aigouy, B., Eaton, S. and Julicher, F. (2007). The influence of cell mechanics, cell-cell interactions, and proliferation on epithelial packing. *Curr. Biol.* **17**, 2095-2104.

Fernández, B. G., Martinez Arias, A. and Jacinto, A. (2007). Dpp signalling orchestrates dorsal closure by regulating cell shape changes both in the amnioserosa and in the epidermis. *Mech. Dev.* **124**, 884-897.

Fox, D. T., Homem, C. C., Myster, S. H., Wang, F., Bain, E. E. and Peifer, M. (2005). Rho1 regulates Drosophila adherens junctions independently of p120ctn. *Development* **132**, 4819-4831.

Franke, J. D., Montague, R. A. and Kiehart, D. P. (2005). Nonmuscle myosin II generates forces that transmit tension and drive contraction in multiple tissues during dorsal closure. *Curr. Biol.* **15**, 2208-2221.

Glickman, N. S., Kimmel, C. B., Jones, M. A. and Adams, R. J. (2003). Shaping the zebrafish notochord. *Development* **130**, 873-887.

Gorfinkiel, N. and Martínez Arias, A. (2007). Requirements for adherens junctions components in the interaction between epithelial tissues during dorsal closure in Drosophila. *J. Cell Sci.* **120**, 3289-3298.

Grevengoed, E. E., Loureiro, J. J., Jesse, T. L. and Peifer, M. (2001). Abelson kinase regulates epithelial morphogenesis in Drosophila. *J. Cell Biol.* **155**, 1185-1198.

Harden, N. (2002). Signaling pathways directing the movement and fusion of epithelial sheets: lessons from dorsal closure in Drosophila. *Differentiation* **70**, 181-203.

Harden, N., Ricos, M., Yee, K., Sanny, J., Langmann, C., Yu, H., Chia, W. and Lim, L. (2002). Drac1 and Crumbs participate in amnioserosa morphogenesis during dorsal closure in Drosophila. *J. Cell Sci.* **115**, 2119-2129.

Hilgenfeldt, S., Erisken, S. and Carthew, R. W. (2008). Physical modeling of cell geometric order in an epithelial tissue. *Proc. Natl. Acad. Sci. USA* **105**, 907-911.

Homem, C. C. and Peifer, M. (2008). Diaphanous regulates myosin and adherens junctions to control cell contractility and protrusive behavior during morphogenesis. *Development* **135**, 1005-1018.

Homsy, J. G., Jasper, H., Peralta, X. G., Wu, H., Kiehart, D. P. and Bohmann, D. (2006). JNK signaling coordinates integrin and actin functions during Drosophila embryogenesis. *Dev. Dyn.* **235**, 427-434.

Hutson, M. S., Tokutake, Y., Chang, M. S., Bloor, J. W., Venakides, S., Kiehart, D. P. and Edwards, G. S. (2003). Forces for morphogenesis investigated with laser microsurgery and quantitative modeling. *Science* **300**, 145-149.

Ingber, D. E. (2006). Mechanical control of tissue morphogenesis during embryological development. *Int. J. Dev. Biol.* **50**, 255-266.

Jacinto, A., Wood, W., Balayo, T., Turmaine, M., Martinez-Arias, A. and Martin, P. (2000). Dynamic actin-based epithelial adhesion and cell matching during Drosophila dorsal closure. *Curr. Biol.* **10**, 1420-1426.

Jacinto, A., Wood, W., Woolner, S., Hiley, C., Turner, L., Wilson, C., Martinez-Arias, A. and Martin, P. (2002a). Dynamic analysis of actin cable function during Drosophila dorsal closure. *Curr. Biol.* **12**, 1245-1250.

Jacinto, A., Woolner, S. and Martin, P. (2002b). Dynamic analysis of dorsal closure in Drosophila: from genetics to cell biology. *Dev. Cell* **3**, 9-19.

Jankovics, F. and Brunner, D. (2006). Transiently reorganized microtubules are essential for zippering during dorsal closure in Drosophila melanogaster. *Dev. Cell* **11**, 375-385.

Kafer, J., Hayashi, T., Maree, A. F., Carthew, R. W. and Graner, F. (2007). Cell adhesion and cortex contractility determine cell patterning in the Drosophila retina. *Proc. Natl. Acad. Sci. USA* **104**, 18549-18554.

Kaltschmidt, J. A., Lawrence, N., Morel, V., Balayo, T., Fernandez, B. G., Pelissier, A., Jacinto, A. and Martinez Arias, A. (2002). Planar polarity and actin dynamics in the epidermis of Drosophila. *Nat. Cell Biol.* **4**, 937-944.

Kiehart, D. P., Galbraith, C. G., Edwards, K. A., Rickoll, W. L. and Montague, R. A. (2000). Multiple forces contribute to cell sheet morphogenesis for dorsal closure in Drosophila. *J. Cell Biol.* **149**, 471-490.

Lamka, M. L. and Lipshitz, H. D. (1999). Role of the amnioserosa in germ band retraction of the Drosophila melanogaster embryo. *Dev. Biol.* **214**, 102-112.

Lecuit, T. and Lenne, P. F. (2007). Cell surface mechanics and the control of cell shape, tissue patterns and morphogenesis. *Nat. Rev. Mol. Cell Biol.* **8**, 633-644.

Liu, R., Woolner, S., Johndrow, J. E., Metzger, D., Flores, A. and Parkhurst, S. M. (2008). Sisyphus, the Drosophila myosin XV homolog, traffics within filopodia transporting key sensory and adhesion cargos. *Development* **135**, 53-63.

Magie, C. R., Pinto-Santini, D. and Parkhurst, S. M. (2002). Rho1 interacts with p120ctn and alpha-catenin, and regulates cadherin-based adherens junction components in Drosophila. *Development* **129**, 3771-3782.

Martin-Bermudo, M. D. and Brown, N. H. (1999). Uncoupling integrin adhesion and signaling: the betaPS cytoplasmic domain is sufficient to regulate gene expression in the Drosophila embryo. *Genes Dev.* **13**, 729-739.

Martinez Arias, A. (1993). Development and patterning of the larval epidermis of Drosophila. In *The Development of Drosophila Melanogaster*, vol. 1 (ed. A. Martinez Arias and M. Bate), pp. 517-607. Cold Spring Harbor, NY: Cold Spring Harbor Laboratory Press.

McBeath, R., Pirone, D. M., Nelson, C. M., Bhadriraju, K. and Chen, C. S. (2004). Cell shape, cytoskeletal tension, and RhoA regulate stem cell lineage commitment. *Dev. Cell* **6**, 483-495.

Millard, T. H. and Martin, P. (2008). Dynamic analysis of filopodial interactions during the zippering phase of Drosophila dorsal closure. *Development* **135**, 621-626.

Murray, M. J., Davidson, C. M., Hayward, N. M. and Brand, A. H. (2006). The Fes/Fer non-receptor tyrosine kinase cooperates with Src42A to regulate dorsal closure in Drosophila. *Development* **133**, 3063-3073.

Narasimha, M. and Brown, N. H. (2004). Novel functions for integrins in epithelial morphogenesis. *Curr. Biol.* **14**, 381-385.

Noble, D. (2008). Genes and causation. *Philos. Transact. A Math. Phys. Eng. Sci.* **366**, 3001-3015.

Noselli, S. (1998). JNK signaling and morphogenesis in Drosophila. *Trends Genet.* **14**, 33-38.

Oda, H. and Tsukita, S. (2001). Real-time imaging of cell-cell adherens junctions reveals that Drosophila mesoderm invagination begins with two phases of apical constriction of cells. *J. Cell Sci.* **114**, 493-501.

Peralta, X. G., Toyama, Y., Hutson, M. S., Montague, R., Venakides, S., Kiehart, D. P. and Edwards, G. S. (2007). Upregulation of forces and morphogenic asymmetries in dorsal closure during Drosophila development. *Biophys. J.* **92**, 2583-2596.
Peralta, X. G., Toyama, Y., Kiehart, D. P. and Edwards, G. S. (2008). Emergent properties during dorsal closure in Drosophila morphogenesis. *Phys. Biol.* **5**, 15004.
Pinheiro, J. C. and Bates, D. M. (2000). *Mixed-Effect Models in S and S-PLUS*. New York: Springer.
Pope, K. L. and Harris, T. J. (2008). Control of cell flattening and junctional remodeling during squamous epithelial morphogenesis in Drosophila. *Development* **135**, 2227-2238.
R Development Core Team (2005). *R: A Language and Environment for Statistical Computing*. Vienna, Austria: The R Foundation for Statistical Computing.
Rauzi, M., Verant, P., Lecuit, T. and Lenne, P. F. (2008). Nature and anisotropy of cortical forces orienting Drosophila tissue morphogenesis. *Nat. Cell Biol.* **10**, 1401-1410.
Reed, B. H., Wilk, R., Schock, F. and Lipshitz, H. D. (2004). Integrin-dependent apposition of Drosophila extraembryonic membranes promotes morphogenesis and prevents anoikis. *Curr. Biol.* **14**, 372-380.
Ring, J. M. and Martinez Arias, A. (1993). puckered, a gene involved in position-specific cell differentiation in the dorsal epidermis of the Drosophila larva. *Development* **Suppl.** 251-259.
Scuderi, A. and Letsou, A. (2005). Amnioserosa is required for dorsal closure in Drosophila. *Dev. Dyn.* **232**, 791-800.
Stronach, B. E. and Perrimon, N. (2001). Investigation of leading edge formation at the interface of amnioserosa and dorsal ectoderm in the Drosophila embryo. *Development* **128**, 2905-2913.
Takahashi, M., Takahashi, F., Ui-Tei, K., Kojima, T. and Saigo, K. (2005). Requirements of genetic interactions between Src42A, armadillo and shotgun, a gene encoding E-cadherin, for normal development in Drosophila. *Development* **132**, 2547-2559.
Toyama, Y., Peralta, X. G., Wells, A. R., Kiehart, D. P. and Edwards, G. S. (2008). Apoptotic force and tissue dynamics during Drosophila embryogenesis. *Science* **321**, 1683-1686.
Trotta, N., Orso, G., Rossetto, M. G., Daga, A. and Broadie, K. (2004). The hereditary spastic paraplegia gene, spastin, regulates microtubule stability to modulate synaptic structure and function. *Curr. Biol.* **14**, 1135-1147.
Wada, A., Kato, K., Uwo, M. F., Yonemura, S. and Hayashi, S. (2007). Specialized extraembryonic cells connect embryonic and extraembryonic epidermis in response to Dpp during dorsal closure in Drosophila. *Dev. Biol.* **301**, 340-349.
Wickman, H. A. (2008). ggplot2: an implementation of the Grammar of Graphics. R package version 0.8.1.
Young, P. E., Richman, A. M., Ketchum, A. S. and Kiehart, D. P. (1993). Morphogenesis in Drosophila requires nonmuscle myosin heavy chain function. *Genes Dev.* **7**, 29-41.

Table S1. Number of extruded cells during dorsal closure

Genotype	Number of AS cells	Number of extruded cells	% Extruded cells
ubiECadGFP	174	19	11
	194	14	7
	161	13	8
	198	16	8
enGal4/UAS-spastin	148	13	9
	149	12	8
	171	12	7
	167	12	7
ASGal4/UAS-p35	233	0	0
	233	0	0
	251	0	0
mys	224	17	8
	218	30	14
	228	16	7
	242	20	8

The total number of cells at the onset of dorsal closure (DC) and the number of extruded cells are indicated for the embryos analysed. There are no significant differences in the percentage of extruded cells between wild-type and enGal4/UAS-spastin embryos (t=0.758, df=6, P=0.48), nor between wild-type and *mys* embryos (t=0.412, df=6, P=0.69).